Available online at www.sciencedirect.com
SCIENCE DIRECT
ELSEVIER
Polymer 47 (2006) 4359–4369
polymer
www.elsevier.com/locate/polymer

Effect of clay on the morphology and properties of PMMA/poly (styrene-*co*-acrylonitrile)/clay nanocomposites prepared by melt mixing

Min Ho Lee [a], Cheol Ho Dan [a], Jeong Ho Kim [a,*], Jaehyug Cha [b], Seonglyong Kim [b], Yongyeon Hwang [b], Chan Hong Lee [b]

[a] *Department of Chemical Engineering, University of Suwon, San 2-2 Wauri, Bongdameup, Hwasung, Kyunggido 445-743, South Korea*
[b] *Performance Polymer Research and Development Institute, LG Chem. Research Park, Daejon, South Korea*

Received 29 October 2005; received in revised form 29 March 2006; accepted 2 April 2006
Available online 2 May 2006

Abstract

Nanocomposites of blends of polymethylmethacrylate (PMMA) and poly(styrene-*co*-acrylonitrile) (SAN) with natural and organically modified montmorillonite clays (Cloisite®25A and Cloisite®15A) were prepared by melt mixing in a twin-screw extruder and the effect of clay on the phase separation morphology and physical properties of nanocomposites was investigated. Multi-pass samples were; those extruded once (one-pass), twice (two-pass) and three times (three-pass). Dispersion of clays in the matrix polymers was investigated using XRD and TEM. Interestingly enough, the clays were observed to be mainly located at the boundaries of PMMA and SAN for most of the nanocomposites. As the number of pass increased, the phase-separated domain size became larger for nanocomposites of PMMA/SAN containing PM, while nanocomposites with clay 25A or 15A showed less degree of growth in domain size in the TEM pictures. Viscosities of the continuous phase and separated domains, and the compatibilizing effect of clays were discussed as the probable explanations for these observations. These were supported by the rheological properties measurements, where the nanocomposites with clay 25A or 15A showed the higher complex viscosities than those of PM and also showed some shear thinning behavior. DSC and TGA analyses were also conducted.

Keywords: Nanocomposite; Clay; Morphology

1. Introduction

In recent years, polymer/clay nanocomposites have been extensively studied, especially on the interfacial phenomena between the silicate layers and polymers in achieving various excellent properties of nanocomposites compared to conventional ones [1–5]. Although polymer/clay nanocomposites have been widely studied using different preparation methods such as in-situ polymerization, solution blending and melt mixing to get the intercalated or exfoliated structures in homopolymers [6–13], there are not many studies reported in the literature on the nanocomposites of polymer blends with clays [14,15]. The influence of clays at the different state of layer separation on the various properties of nanocomposites is largely related to their interaction behavior at the interface with polymers. In this regard, it becomes more complicated and even more interesting when it comes to the nanocomposites of polymer blends with clays since, there are more interfaces involved in this case than nanocomposites of one polymer and the clay.

In the previous studies in the literature, clays are reported to be intercalated or exfoliated in PMMA nanocomposites depending on the preparation methods [16–18]. Nanocomposites of poly(styrene-*co*-acrylonitrile) (SAN) with clays are also reported in the literature where clays are observed to be intercalated in SAN matrices [19–21]. It is well known that the mixture of PMMA and SAN forms a miscible blend and the origin of miscibility of PMMA/SAN blends has been suggested to be the repulsion effect between styrene and acrylonitrile units in SAN. It means that the miscibility of the blend is not very strong compared to the ones with specific interactions between the blend components [22,23]. PMMA is reported to be miscible with SAN depending on the AN composition in the range from 9.4 up to 34.4 wt% of AN in SAN [24–30]. PMMA/SAN blends show the lower critical solution temperature (LCST) behavior. The cloud point for 50/50 blend is reported to be around 180 °C [31], which is below the usual melt processing temperature of PMMA or SAN. Even though there

* Corresponding author. Tel.: +82 31 220 2450; fax: +82 31 220 2528.
E-mail address: jhkim@suwon.ac.kr (J.H. Kim).

0032-3861/$ - see front matter © 2006 Elsevier Ltd. All rights reserved.
doi:10.1016/j.polymer.2006.04.003

is a report in the literature that shear induced mixing can raise the cloud point a little bit [32], our processing temperature, 230 °C, was still above the phase separation temperature of the PMMA/SAN blend. Therefore, the phase separation occurs during melt processing when PMMA and SAN is melt mixed with clay in the extruder.

In this study, nanocomposites of PMMA/SAN blend with natural and organically modified montmorillonite clays were prepared by melt processing in the twin-screw extruder and the effect of clay on the phase separation and physical properties of nanocomposites was investigated. Montmorillonites used were pristine montmorillonite (Cloisite®Na^+) in natural form and modified clays (Cloisite®25A and Cloisite®15A) with cationic modifiers, such as alkyl ammoniums. Analyses were carried out using X-ray diffraction (XRD), transmission electron microscopy (TEM), differential scanning calorimetry (DSC), thermogravimetric analysis (TGA) and modular compact rheometer (MCR) to investigate the dispersion of clay and its influence on the physical properties of nanocomposites.

2. Experimental

2.1. Materials

The polymers used in this study were PMMA (LG Chem., melt index: 5.8) and SAN (AN content: 26 wt%, LG Chem., melt index: 10). Pristine montmorillonite, Cloisite Na^+ (PM) was obtained from Southern Clay Products, which has cation-exchange capacity (CEC) of 92.6 mequiv./100 g clay. Organically modified montmorillonite, Cloisite 25A (CEC: 95 mequiv./100 g) and Cloisite 15A (CEC: 125 mequiv./100 g) were also obtained from Southern Clay Products. Cloisite 25A and 15A are montmorillonites modified with a dimethyl, hydrogenated tallow, 2-ethylhexyl quaternary ammonium ion, and dimethyl, dehydrogenated tallow quaternary ammonium ion, respectively. PM has the highest hydrophilicity and 15A has the lowest, while clay 25A is located between the two.

2.2. Preparation of PMMA/SAN/clay nanocomposites

All clays were dried prior to use for 24 h in the vacuum oven to remove any moistures. PMMA and SAN were also dried for 4 h at 80 °C before blending in the extruder. The clay loading of all nanocomposite samples was set at 5 wt% based on inorganic clay contents excluding any surfactant content in the organically modified clays, such as 25A and 15A. PMMA, SAN and clays were fed into the extruder at the same time and melt mixed in the twin-screw extruder (Bautek corp. BA-19ST) to prepare nanocomposites at processing temperatures varying from 200 to 230 °C depending on the position in the extruder. The extrudates from the extruder were pelletized and injection molded in the mini-injection molding machine (Bautek corp.) into the test specimens. To investigate the effect of number of passes (longer residence time in the extruder with more pass), some of the extrudates from the extruder were re-fed into the extruder again to prepare the multi-pass samples such as two-pass and three-pass samples in this study. Samples thus prepared were listed in Table 1.

2.3. Characterization and measurements

The silicate interlayer distance in the polymer matrix was obtained using an X-ray diffraction pattern from X-ray diffractometer (D-8 Advance, Cu radiation $\lambda = 0.154$ nm) at 40 kV, 35 mA. TEM images of nanocomposite specimens were obtained using energy filtering transmission electron microscopy (EM-912 OMEGA, Carl Zeiss Co.) with operating voltage of 120 kV at the Korea Basic Science Institute. TEM specimens were prepared by encapsulating nanocomposites in the epoxy resin and microtoming at room temperature. The thermal properties of nanocomposites were measured by differential scanning calorimetry (DSC, TA Instrument DSC 2010) at a heating rate 20 °C/min in nitrogen atmosphere. The second scan was taken for analysis after first scan followed by rapid cooling. Thermogravimetric analysis (TGA, NETZSCH) was conducted under nitrogen atmosphere at a heating rate of 10 °C/min. The complex viscosity measurement was

Table 1
Composition and number of extrusion (pass) of PMMA/SAN nanocomposites

Sample designation	Polymer and clay composition (wt%)[a]					Number of extrusion (pass)
	PMMA	SAN	PM	25A	15A	
P/S-1	50	50	–	–	–	1
P/S-2	50	50	–	–	–	2
P/S-3	50	50	–	–	–	3
P/S–PM-1	47.5	47.5	5	–	–	1
P/S–PM-2	47.5	47.5	5	–	–	2
P/S–PM-3	47.5	47.5	5	–	–	3
P/S-25A-1	47.5	47.5	–	5	–	1
P/S-25A-2	47.5	47.5	–	5	–	2
P/S-25A-3	47.5	47.5	–	5	–	3
P/S-15A-1	47.5	47.5	–	–	5	1
P/S-15A-2	47.5	47.5	–	–	5	2
P/S-15A-3	47.5	47.5	–	–	5	3

[a] Clay compositions are based on inorganic clay contents.

performed on MCR 300 with parallel plate geometry of 25 mm in diameter. Dynamic frequency sweep test were conducted at 220 °C with angular frequency ranging from 0.01 to 100 rad/s.

3. Results and discussion

3.1. Effect of differently modified clay and of number of passes on the clay dispersion and phase separation

XRD results for PMMA/SAN with PM clays (P/S–PM) are shown in Fig. 1(a), where the 2θ values can give some information on the interlayer distance of the clay. The d-spacing was calculated using Bragg's equation ($n\lambda = 2d\sin\theta$), where λ is the wavelength of the X-ray, d is the interlayer distance and θ is the angle of incident radiation. The result of calculation is listed in Table 2. The 2θ value of P/S–PM after one-pass, 7.06° ($d = 1.25$ nm) was not much different from that of PM, 7.54° (1.17 nm) but those after two-pass and three-pass decreased to about 2.91° (3.03 nm) and 2.60° (3.39 nm), respectively, showing that the d-spacing was increased. This observation can be interpreted as a result of shearing of clays under repeated processing and longer residence time in the extruder. It also agrees with the previous observations in the literatures that clays can be intercalated in PMMA [11] or SAN [19]. On the other hand, the 2θ value of P/S-25A in Fig. 1(b) decreased to 2.95° (3.0 nm) from 4.86° (1.81 nm) of pure clay 25A immediately after one-pass and remains around the same after two-pass or three-pass. But the intensity of the peak around 2.95° decreased substantially after three-pass showing a very good dispersion after three-pass. XRD results of nanocomposites with clay 15A (Fig. 1(c)) shows that the peak position at $2\theta = 2.60°$ (3.39 nm) of pure clay 15A decreased very little with increasing number of passes while the intensity of this peak decreased very much after three-pass comparable to that of the nanocomposite with 25A after three-pass. This observation may lead to the speculation that the interlayer distance of the clay was maintained at around the same as that of clay 15A itself, but only the thickness of individual clay particles decreased by delamination due to shear with increasing processing. In other words, the number of layers in each clay particle decreased with increasing number of pass. This may be supported by the TEM results that more clay particles are seen in the TEM images with increasing number of passes, which will be discussed again later in the TEM analysis. It is noted here that the 2θ values after three-pass for nanocomposites with all clays are around 3°, PM = 3.39°, 25A = 3.00°, 15A = 3.46°, but these numbers cannot be said to be exact since, their maximum peak positions are not unambiguous depending on observers. Judging only from theses XRD results, PMMA/SAN nanocomposites can be said to show some intercalation. In studying the nanocomposites, the difficulty is that no single characterization technique can adequately describe the state of clay dispersion in the composite; the combined characterization methods are necessary and especially TEM is proved to be quite effective. In this regard, TEM pictures were taken for all samples investigated.

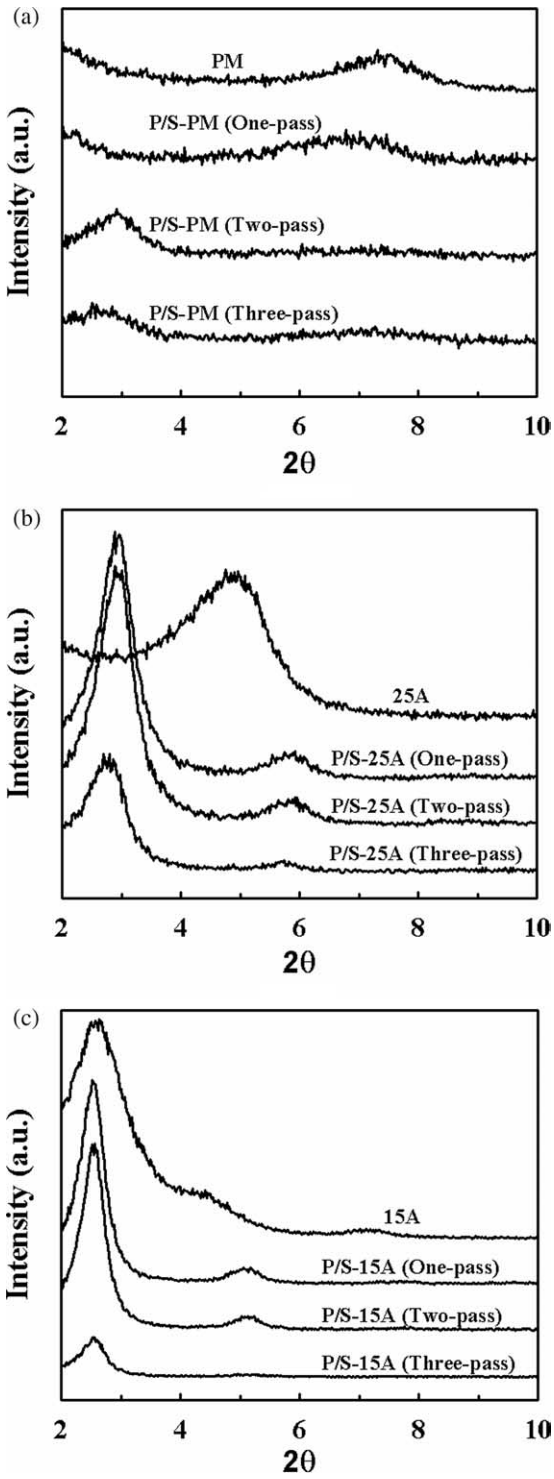

Fig. 1. X-ray diffraction patterns of PMMA/SAN/clay nanocomposites.

Fig. 2(a)–(c) shows the TEM images of PMMA/SAN blend without any clay after one-, two- and three-pass, respectively. The phase-separated domains and continuous phase morphology are clearly observed from these pictures. This is quite natural since, the PMMA/SAN forms a miscible blend at room temperature and begin to phase separate above 180 °C at 50 wt% SAN content. In this study, PMMA and SAN were melt-blended in the twin-screw extruder at 230 °C. Upon

Table 2
XRD results for PMMA/SAN nanocomposites

Samples	2θ value (°)	d-Spacing (nm)
Clay PM	7.54	1.17
P/S–PM-1	7.06	1.25
P/S–PM-2	2.91	3.03
P/S–PM-3	2.60	3.39
Clay 25A	4.86	1.81
P/S-25A-1	2.95	3.00
P/S-25A-2	2.95	3.00
P/S-25A-3	2.76	3.19
Clay 15A	2.60	3.39
P/S-15A-1	2.54	3.47
P/S-15A-2	2.54	3.47
P/S-15A-3	2.55	3.46

melting in the extruder, they may form a miscible blend at the beginning followed by immediate phase-separation due to the high processing temperature. In this image, bright area is PMMA and dark one represents SAN. After two-pass, the elongated domain shape is observed which may be due to the shear in the extruder. After three-pass, bright domains appeared to be more agglomerated than those of two-pass which may be the result of progress in phase separation.

Fig. 3 shows the TEM pictures of PMMA/SAN nanocomposites with 5 wt% PM (natural clay) depending on the number of passes in the extruder. First, the size of the bright domain increased with increasing number of passes. Secondly, the domain size is much smaller than the one in corresponding TEM pictures of PMMA/SAN without clay in Fig. 2. In the image of the one-pass sample (P/S–PM-1) in Fig. 3(a), a few clays are seen in this 500 nm magnification with the big tactoids of clays in some areas. But, in the TEM image of the two-pass sample (P/S–PM-2) of Fig. 3(b), much more clays are observed in this picture. This means that PM clays start to be dispersed due to shear with more passes, which provide longer mixing time since, clay dispersion in melt mixing is largely a kinetic process. One very interesting and even remarkable feature in this picture is that most of the clays are observed to be located at the boundaries between PMMA and SAN, and some of the remaining are inside the PMMA domain which is notable in the 250 nm magnification images of two-pass and three-pass nanocomposites in Fig. 4(a) and (b), respectively. Similar behavior of clays preferentially segregating to the interface and some dispersed in the matrix was previously reported in polypropylene/ethylene–propylene rubber (EPR)/clay nanocomposites by Mirabella [10]. Inclusion of clays in the dispersed domains may cause an increase in the viscosity of those domains. This can contribute to some extent to an increase in dispersed PMMA domain size with increasing number of passes, which is observed in images in Fig. 3, since, the continuous phase cannot give enough shear to dispersed domains due to their relatively low viscosity compared to that of dispersed ones. Similar reasoning concerning the effect of clay on the melt viscosity was also mentioned in the same study by Mirabella [10]. In the high magnification (50 nm) picture of the three-pass sample in Fig. 5, the location of clay at the boundaries of PMMA and SAN becomes more profound and

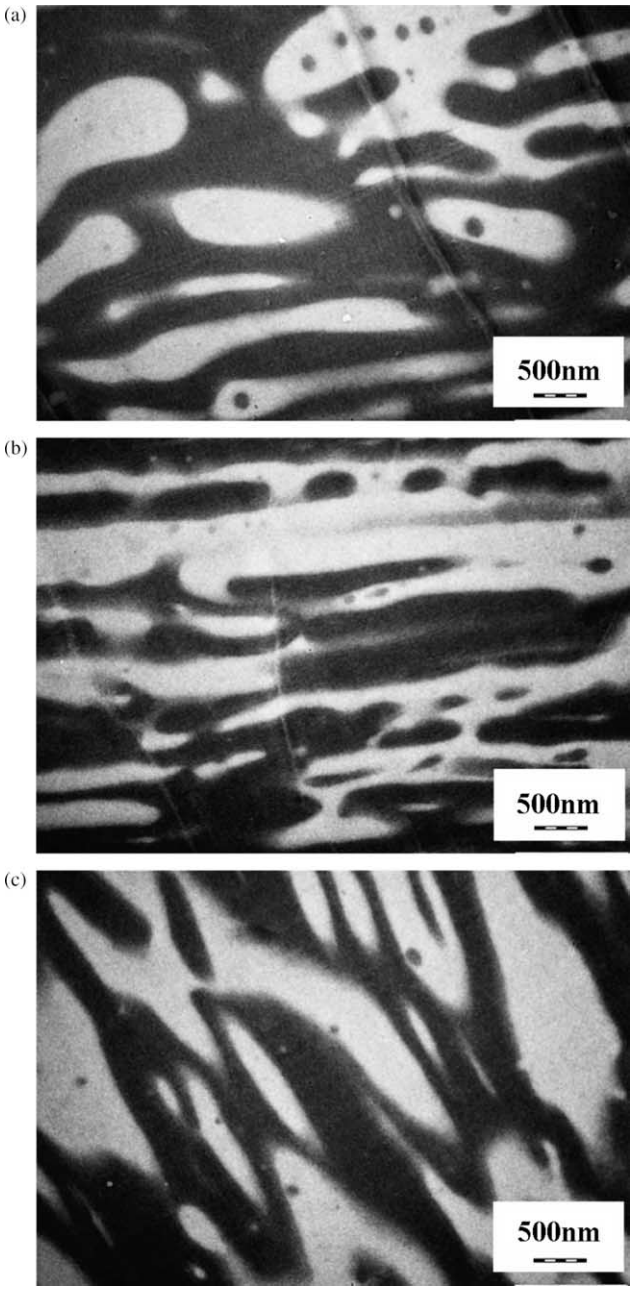

Fig. 2. TEM images of PMMA/SAN without clay (500 nm scale) prepared by (a) one-pass, (b) two-pass and (c) three-pass processing in the extruder.

the intercalation and even some degree of exfoliation of clay is observed here. About 4–5 clay layers in one clay particle are observed in the picture and the distance between two layers in this image is measured to be around 2.1 nm, which is lower than that obtained from XRD result (3.39 nm), but still higher than that of pure clay (1.17 nm). At this point, the reason why most of the clay particles are located at the boundaries and some are inside the dispersed domain is not clear, but some possibilities may be given. First, the hydrophilic nature of clays prevent them from residing in either phases of separated domains of polymers which are less hydrophilic than clays, for which reason most of the clays are at or near the boundaries of phase-separated domains. Secondly, the next question is why

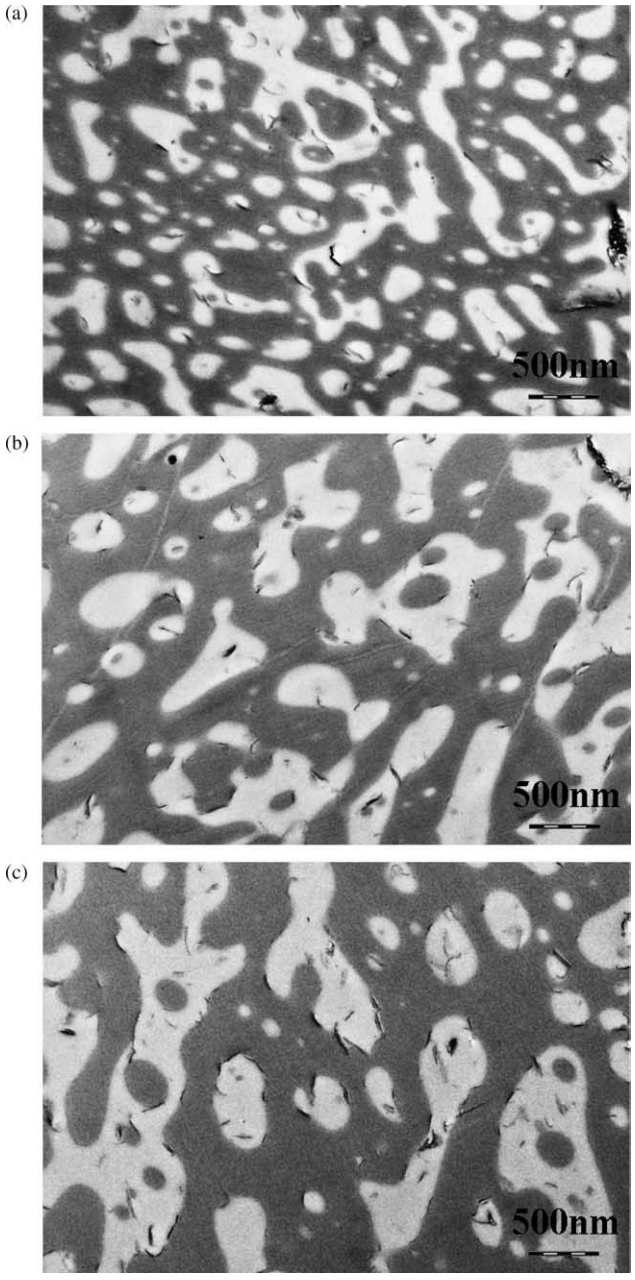

Fig. 3. TEM images of PMMA/SAN with 5 wt% PM (500 nm scale) prepared by (a) one-pass, (b) two-pass and (c) three-pass processing in the extruder.

some of the clays are in the PMMA domains. As mentioned in the previous section, the miscibility of PMMA and SAN may be due to the intramolecular repulsion rather than the favorable intermolecular interaction and it follows that their miscibility is rather weak resulting in low cloud points compared to other miscible blends. Therefore, the nature of two polymers may be somewhat different and the PM clay has more affinity to PMMA than SAN. Nanocomposites of PMMA with PM and those of SAN with PM were prepared and the glass transition temperature (T_g) were measured. The result showed that there was a change in T_g of PMMA with PM, while almost no change was observed for SAN with PM, which may be another indirect evidence that PMMA is more affected by PM. Also, it is noted

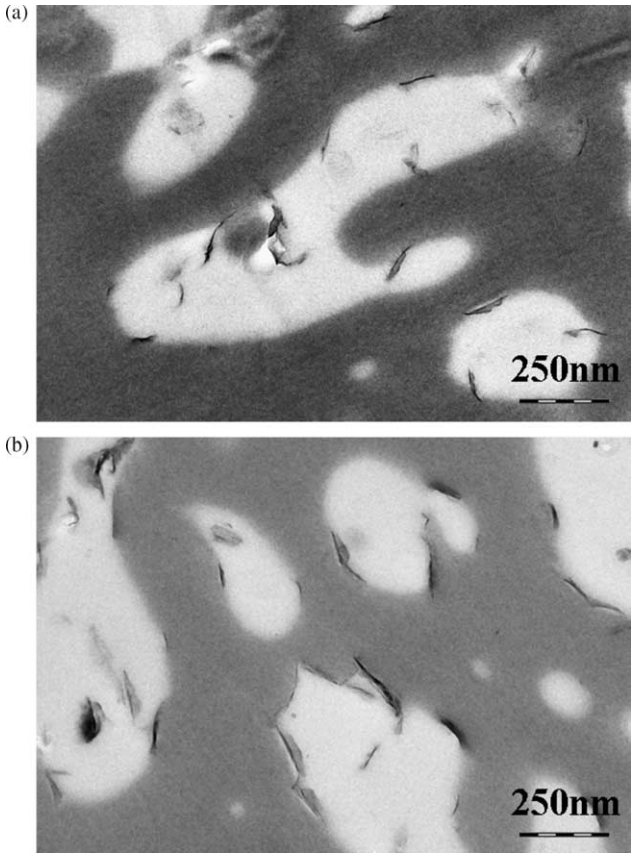

Fig. 4. TEM images of PMMA/SAN with 5 wt% PM (250 nm scale) prepared by (a) two-pass and (b) three-pass processing in the extruder.

that PM, natural clay without any modification still appeared to show some intercalated structures after two- or three-pass processing and the interlayer distance increased a little bit. It is not surprising since, PMMA and SAN have some hydrophilic nature although they are not very similar to PM. Since, shear cannot be delivered to clay without some affinity between clay and polymer matrix, PM may have some affinity to PMMA or SAN. The shear may cause delamination of the clay layer from the outside layer as proposed by Jana [8]. Actually, some single

Fig. 5. TEM image of PMMA/SAN with 5 wt% PM (50 nm scale) prepared by three-pass processing in the extruder.

layers of PM are observed in the TEM image of one-pass sample in Fig. 3(a).

For nanocomposites with clay 25A (samples P/S-25A-1,2,3), the first thing to be noted in Fig. 6 is that the phase-separated domain sizes in all passes are smaller than those of nanocomposites with PM and those domain sizes do not change noticeably with increasing number of passes as can be seen from Fig. 6(a)–(c). Secondly, much more dispersion of clays was observed from the one-pass sample through three-pass samples. Also, much more clay particles are observed in Fig. 6(a) and (b) than those in nanocomposites containing PM in Fig. 3(a)–(c). This may be partly due to the better dispersion of clay 25A in the blend. Here again, the clay particles are located mainly at or near the boundaries of PMMA and SAN, except that some of the clays are within the continuous dark zone also as well as in the bright area, which is a little different behavior from nanocomposites with PM. This seems to be due to the modifier in the clay, which makes the nature of the clay surface different than natural clay, PM. 25A is more hydrophobic than PM although it may be still regarded to have some hydrophilic nature due to the clay surface not covered by the modifier. This little change in the domain size with increasing number of pass may be interpreted in two aspects. One is the viscosity of the continuous phase where some of the clay particles are located. Due to the existence of clay particles also in the continuous phase, the viscosity of this continuous phase increases to some extent and this highly viscous continuous phase may prevent the coagulation of the domains with the progress of phase separation and thereby prevent the growth of the domain size. Another aspect, which may be feasible is that the clay acts as a compatibilizer between PMMA and SAN. By arranging themselves at the boundaries of the two polymers, clay stabilizes the phase morphology and stays the same through the phase separation process. It is not certain at this stage which of the two scenarios is more feasible. Compatibilizing effect of clay was also mentioned in the polypropylene/EPR/clay study [10]. It is quite clear from TEM image of one-pass sample (250 nm magnification) in Fig. 7 that the clay particles are mostly located at or near the boundaries from the one-pass samples. Further, magnified images (50 nm magnification) in Fig. 8 show that the number of clay layers in one particle is mostly 4–7 for one-pass sample (Fig. 8(a)) while that of two-pass sample (Fig. 8(b)) is mostly 2–4. If most of the clays are intercalated and almost exfoliated into particles with two or three layers as in Fig. 8(c), then the modifiers, which were originally present in 25A might be released into the matrix of PMMA and SAN. This may cause the lowering of the glass transition temperature of the polymer matrix, which is really the case observed in DSC analysis. This will be discussed more in Section 3.2.

Fig. 9 shows the TEM images of nanocomposites with clay 15A. Overall shape and sizes of domains in the images look

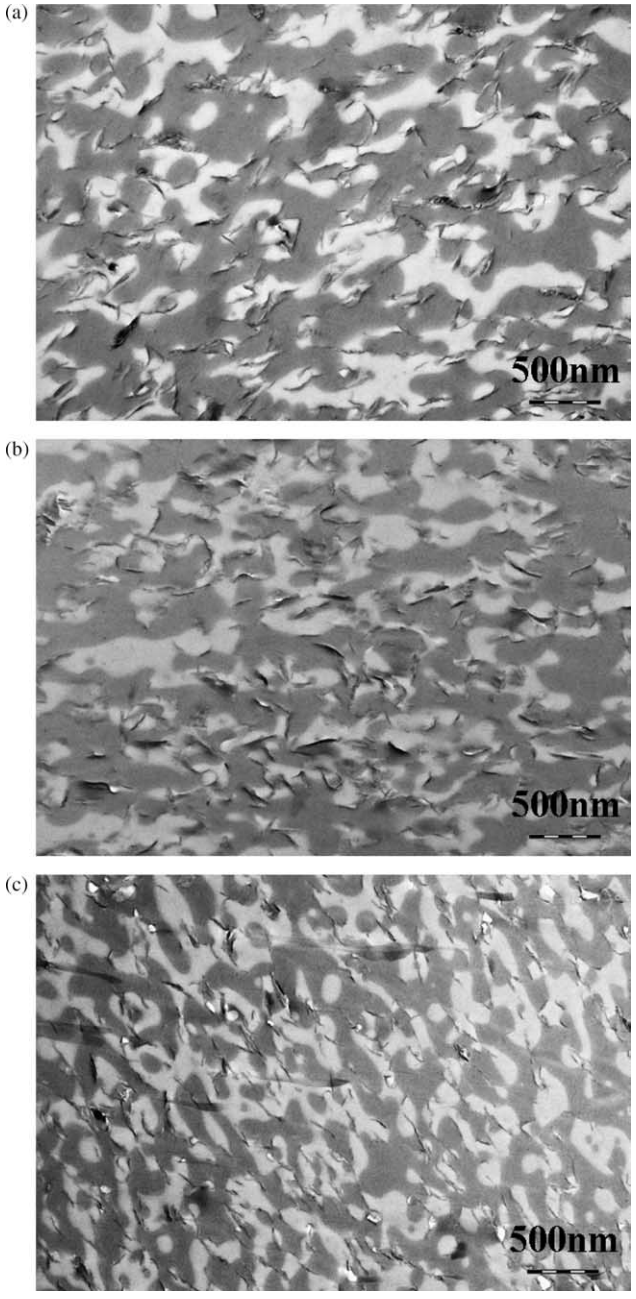

Fig. 6. TEM images of PMMA/SAN with 5 wt% 25A (500 nm scale) prepared by (a) one-pass, (b) two-pass and (c) three-pass processing in the extruder.

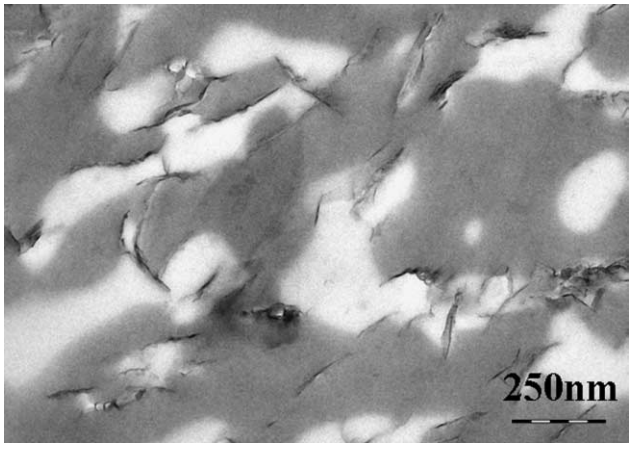

Fig. 7. TEM image of PMMA/SAN with 5 wt% 25A (250 nm scale) prepared by one-pass processing in the extruder.

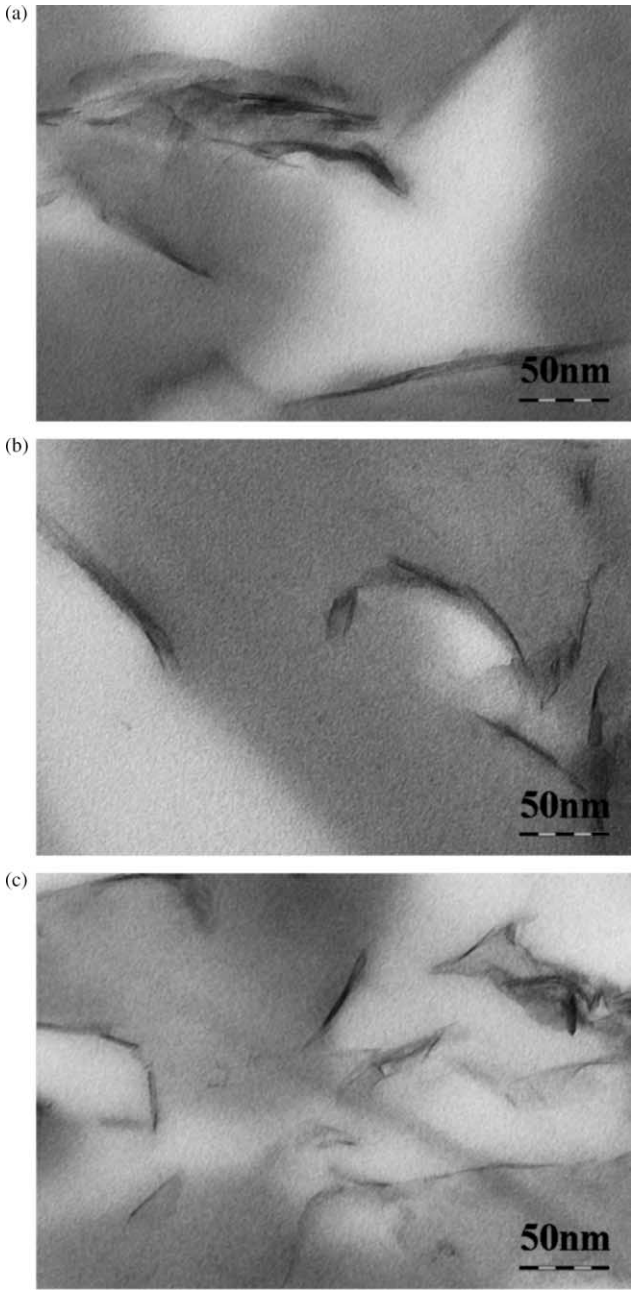

Fig. 8. TEM images of PMMA/SAN with 5 wt% 25A (50 nm scale) prepared by (a) one-pass, (b) two-pass and (c) three-pass processing in the extruder.

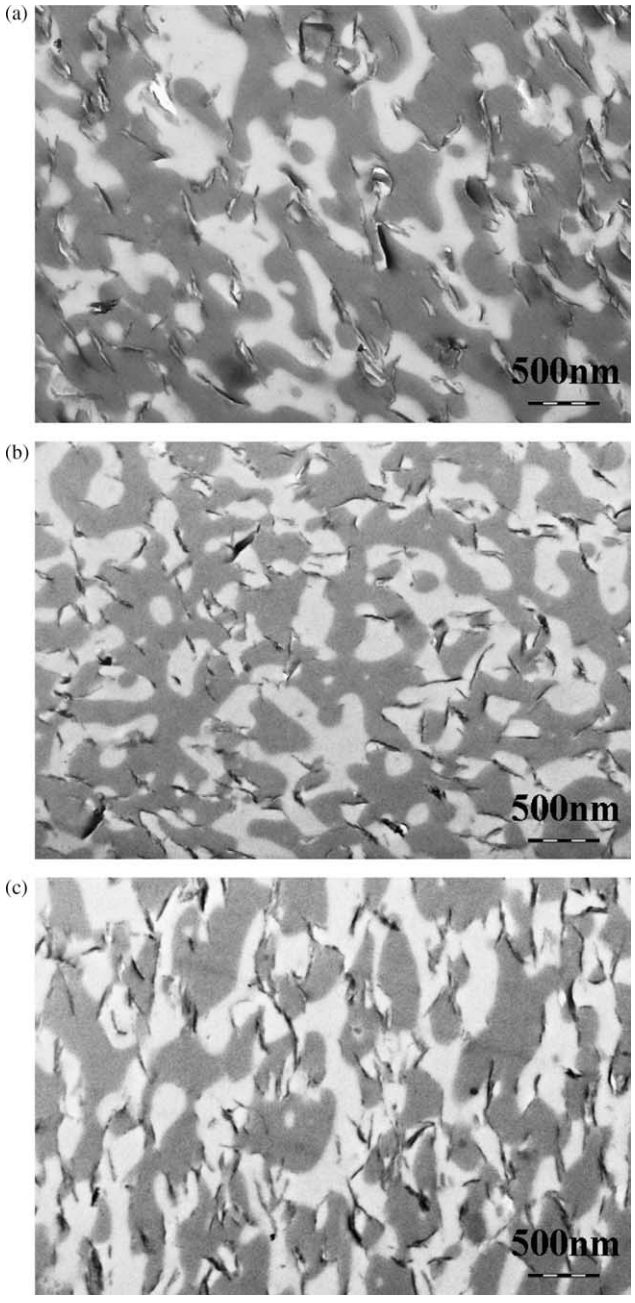

Fig. 9. TEM images of PMMA/SAN with 5 wt% 15A (500 nm scale) prepared by (a) one-pass, (b) two-pass and (c) three-pass processing in the extruder.

similar to those of 25A in Fig. 6, but the domain sizes are generally a little bit larger than those of nanocomposites with 25A. The difference between 25A and 15A is that 15A has longer chain at one branch of quaternary ammonium ion in the modifier than 25A and also, 15A has a larger modifier concentration so that more clay surface of 15A is covered with modifier and even some excess modifier can be present at the clay surface. Clay 15A may be regarded as almost hydrophobic in nature since, almost no pure inorganic clay surface may be exposed to polymer. In the higher magnification (250 nm) image for one-pass sample in Fig. 10, most clays are again observed to be located near the boundaries. One thing to be noted is that there is not much change in the thickness of the clay particles from one-pass to three-pass as observed in Fig. 11(a) through (c). Judging from above XRD and TEM results, it may be concluded that clays 25A and 15A are better dispersed than PM after one-pass while it became similar after three-pass. Nanocomposites with 25A show a smaller domain sizes than those with 15A or PM. This may be explained either in terms of balance of viscosities between two separate domains, or in thermodynamic sense, the balance between platelet spacing caused by modifier, level of access to exposed silicate surface and number of unfavorable interaction between the polymer and the alkyl units of modifier as proposed by Paul et al. [33]. Clay 25A has about the same ion exchange capacity (95 mequiv./100 g clay) with PM

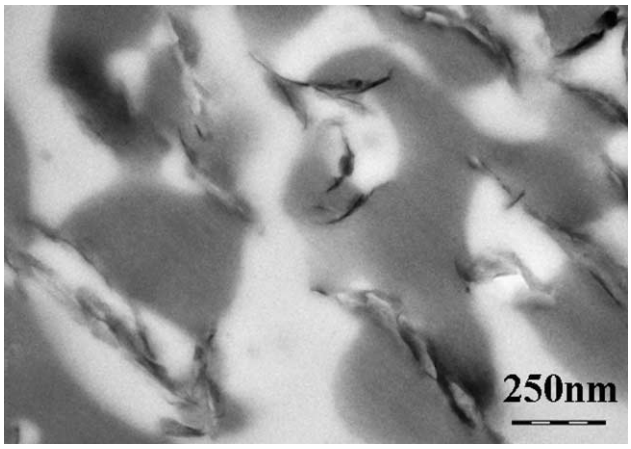

Fig. 10. TEM image of PMMA/SAN with 5 wt% 15A (250 nm scale) prepared by one-pass processing in the extruder.

(92.6 mequiv./100 g clay) and probably does not possess much excess modifier than 15A, although there may be still some unexchanged Na^+. This may leave some surface of the hydrophilic clay exposed to polymer and the balance of this hydrophilic surface and the hydrophobic modifier makes 25A more similar to the nature of PMMA and SAN. This may be another manifestation of the reports that interaction between clay and polymer can be more important than that between modifier and polymer in clay dispersion [34,35]. Although there is a report in the literature that the modifiers existing in excess of the ion exchange capacity of natural clay (PM) reside primarily in the interlayer, not on the outer surface of clay [36], the possibility that some of the excess modifier can still exist outside the surface of the clay cannot be excluded completely, especially when the excess amount is significant such as 15A (125 mequiv./100 g clay) in this study. In the latter case, the outer surface of the clay is mostly covered by the hydrophobic modifier and the affinity of the modified clay with PMMA and SAN becomes weak. Of course, the modifiers in both 25A and 15A increase the gallery height and make the layer separation much easier by shear from extruder since, the modifier inside the layer weakens the electrostatic force between silicate layers compared to PM, which is already proved in this study that 25A and 15A show a good dispersion from the one-pass samples.

3.2. Thermal properties of PMMA/SAN/clay nanocomposites

The criterion for miscibility frequently used in DSC analysis is the appearance of a single glass transition temperature (T_g) in the blend. But since, PMMA and SAN both have the similar glass transition temperatures such as 102 °C for PMMA and 105 °C for SAN in the present study, it is hard to judge the miscibility from DSC results. Still some useful information on the phase behavior can be obtained from DSC analysis. DSC thermograms of nanocomposites of PMMA/SAN with 25A depending on the number of pass are shown in Fig. 12 as an example and actually a single transition was observed for all samples tested. The onset of transition was taken as T_g of the nanocomposite and the width of transition between the onset

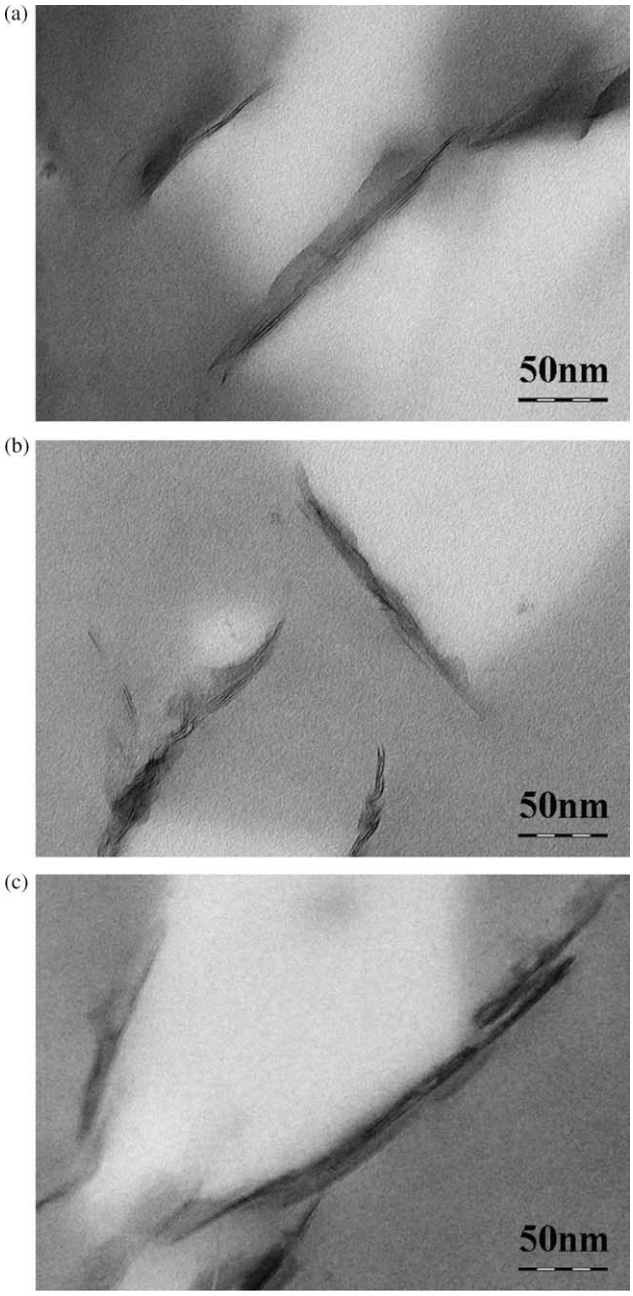

Fig. 11. TEM images of PMMA/SAN with 5 wt% 15A (50 nm scale) prepared by (a) one-pass, (b) two-pass and (c) three-pass processing in the extruder.

and the end of transition temperatures was considered to be ΔT_g of transition. These data are listed in Table 3. For PMMA/SAN blend without any clay (P/S-1,2,3), T_g decreased with increasing pass from 105.5 to 102.3 °C and at the same time the ΔT_g increased from 9.2 to 11.5 °C. This increase in ΔT_g and the decrease in T_g, although they are rather small, can be thought to originate from the phase separation with increasing number of processing. For nanocomposites with PM, glass transition temperature became higher with increasing number of passes, which may be due to the better dispersion of clay with more mixing. They showed a smaller ΔT_g compared to the ones without clay. Nanocomposites with clays 25A and 15A showed slight decrease in T_g with increasing number of pass. This is not

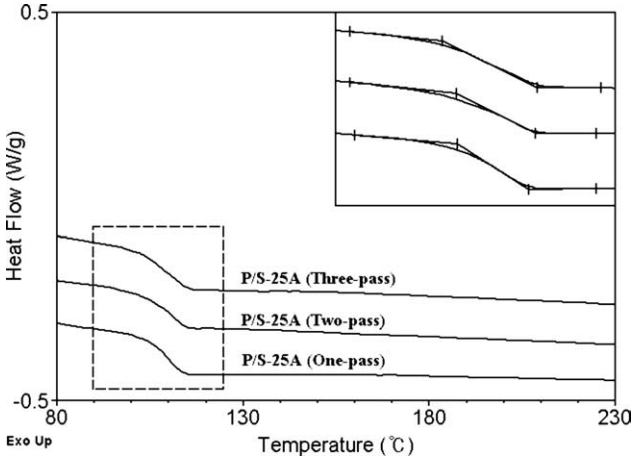

Fig. 12. DSC thermograms of P/S-25A prepared by one-, two- and three-pass processing in the extruder.

Table 3
T_g and ΔT_g of PMMA/SAN nanocomposites

Samples	T_g (°C)	ΔT_g (°C)
P/S-1	105.5	9.2
P/S-2	104.1	10.9
P/S-3	102.3	11.5
P/S–PM-1	106.1	7.9
P/S–PM-2	106.2	8.3
P/S–PM-3	107.2	8.2
P/S-25A-1	105.0	8.8
P/S-25A-2	104.8	9.9
P/S-25A-3	103.1	11.8
P/S-15A-1	105.6	8.9
P/S-15A-2	104.2	9.3
P/S-15A-3	104.0	8.9

surprising, since, clays 25A and 15A have low molecular weight modifiers in them and these modifiers are known to be degraded above 200 °C by Hoffmann elimination reaction [35] which can contribute to lowering of glass transition temperatures of the nanocomposites. One clear difference in T_g behavior of the nanocomposites with clays from those without clay is the width of transition. There is very little change in ΔT_g for the nanocomposites containing clays with increasing number of processing except for the ones containing clay 25A. Whether this little change in ΔT_g can be regarded as some indirect evidence of retardation of the phase separation by clays due to the viscosity increase or due to the thermodynamic effect remains to be the subject of further investigation. Actually, the magnitudes of change in T_g or ΔT_g are relatively small, so it is with extreme caution that any conclusions are drawn on the phase separation rate with the addition of clay at this stage. For nanocomposites with clay 25A, the unexpected increase in the width of transition after three-pass is not quite clear but may be due to the good dispersion of clay in the polymer matrix. More modifiers may be released from the clay and mixed with the matrix polymer resulting in the lowering of T_g representing the low onset of T_g, while in some area, more clay platelets meet the matrix polymer giving high end of T_g.

Table 4
Thermogravimetric results for PMMA/SAN nanocomposites

Samples	$T_{10\%}$ (°C)[a]	T_{max} (°C)[b]
P/S-1	360	400
P/S-2	366	400
P/S-3	366	398
P/S–PM-1	364	403
P/S–PM-2	365	401
P/S–PM-3	371	404
P/S-25A-1	370	405
P/S-25A-2	374	407
P/S-25A-3	368	401
P/S-15A-1	362	403
P/S-15A-2	364	402
P/S-15A-3	363	402

[a] $T_{10\%}$, temperature at which 10% of weight loss occurs.
[b] T_{max}, temperature at which the TGA curve shows the maximum slope.

TGA results for nanocomposites after one-, two- and three-pass processing are given in Table 4. It shows that nanocomposites with clay 25A give the highest improvement in thermal stability although the degree of improvement is not remarkable in all cases. DSC and TGA results generally agree with the analysis of XRD and TEM results.

3.3. Rheological properties of PMMA/SAN/clay nanocomposites

The plots of $|\eta^*|$ vs. ω for PMMA/SAN without and with clays PM, 25A and 15A after one-, two- and three-pass are shown in Fig. 13(a)–(c). Blends of PMMA/SAN without clay and nanocomposites with PM exhibited the similar behavior where they showed almost Newtonian behavior at low ω at all cases of one-, two- and three-pass, while those with 25A or 15A showed higher complex viscosity than those with PM at low frequency. Clays may be thought to impart some resistance to flow. This means that the dispersion of clay in nanocomposites with 25A or 15A is better than those with PM. This kind of behavior in complex viscosity for better clay dispersion was previously observed in the other studies [37,38]. Especially, it is noted that nanocomposites with 25A maintained the high complex viscosity at low ω even after three-pass as shown in Fig. 13(c), while the complex viscosity of nanocomposites with clay 15A decrease with the increasing number of pass. This again implies that the dispersion of clay 25A is better than that of clay 15A. The difference of complex viscosity between nanocomposites with 25A and those with 15A was very small after one-pass but becomes substantial after three-pass. This again is consistent with the previous results that nanocomposites with 25A showed the better dispersion of clay and smaller domain sizes than those with 15A.

Fig. 14 shows the plot of $|\eta^*|$ vs. ω for nanocomposites with 25A after one-, two- and three-pass processing. The complex viscosity was observed to even increase with increasing number of pass, though again the magnitude was quite small, which again means the good dispersion of clay 25A with more processing.

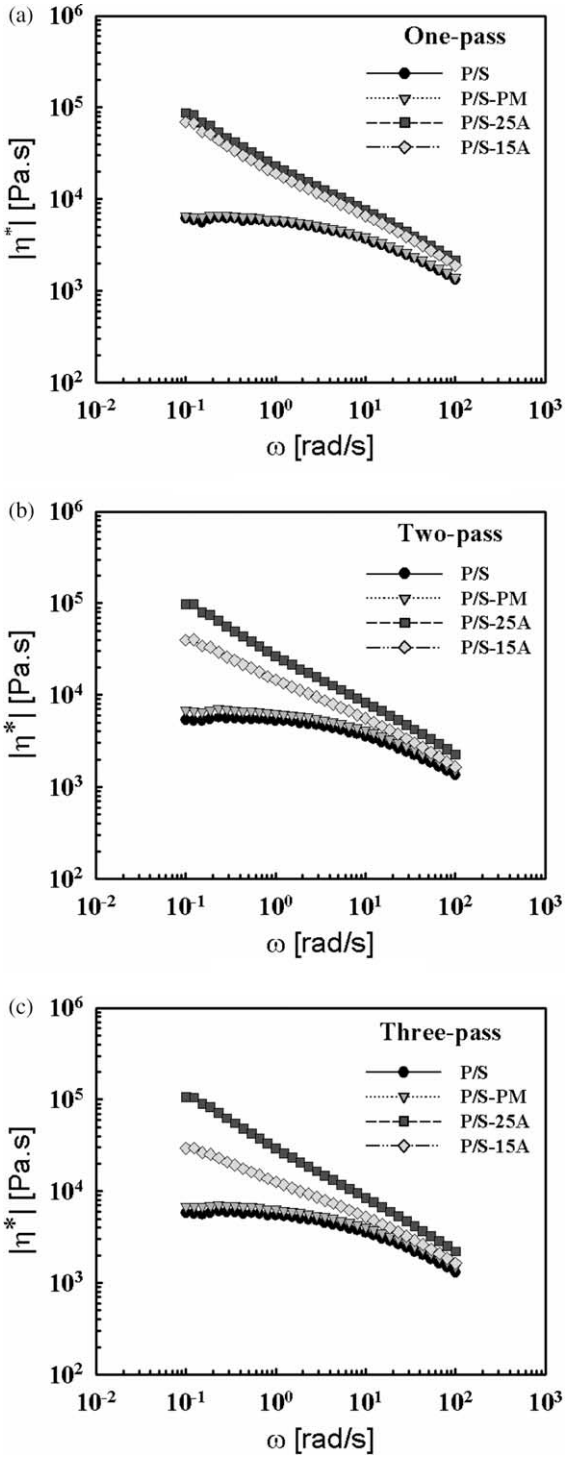

Fig. 13. Plots of $|\eta^*|$ vs. ω for PMMA/SAN without clay and nanocomposites with clays PM, 25A and 15A after (a) one-pass, (b) two-pass and (c) three-pass.

4. Conclusion

Nanocomposites of PMMA and SAN without any clay and with three different clays (Cloisite®Na^+ (PM), Cloisite®25A and 15A) were melt-processed in the twin-screw extruder. Multi-pass samples were prepared such as those extruded once (one-pass), twice (two-pass) and three times (three-pass).

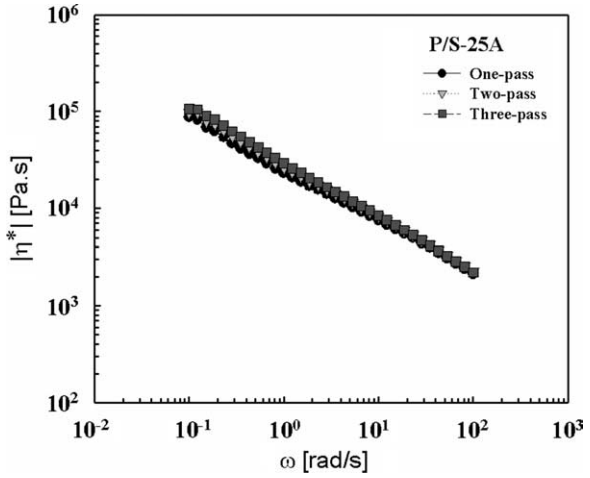

Fig. 14. Plots of $|\eta^*|$ vs. ω for PMMA/SAN nanocomposites with clay 25A after one-, two- and three-pass.

Dispersion of clays in the matrix polymers was investigated using XRD and TEM. In the nanocomposites containing PM, the clays were observed to be mainly located at the boundaries of PMMA and some of them in PMMA domains. As the number of pass increased, the phase-separated domain size became larger and the DSC result for this nanocomposite shows lowering in glass transition temperature and widening of glass transition region. Nanocomposites with 25A or 15A showed less degree of growth in domain size in the TEM pictures and little change in T_g and the widths of transition with increasing number of passes in DSC thermograms. Clay 25A appeared to show a better dispersion in the matrix. Viscosities of the continuous phase and separated domains, and the compatibilizing effect of clays are discussed as the possible explanation for these observations. These results are also supported by the DSC and the rheological property measurements.

Acknowledgements

Financial support from LG Chem. is greatly appreciated. We thank Prof L.A. Goettler at University of Akron for the helpful discussions. We acknowledge the efforts of the Korea Basic Science Institute for taking very nice TEM pictures.

References

[1] Messersmith PB, Giannelis EP. Chem Mater 1994;6:1719–25.
[2] Kojima Y, Usuki A, Kawasumi M, Okada A, Fujushima A, Kurauchi T, et al. J Mater Res 1993;8:1185–9.
[3] Mirabella Jr FM. Dekker encyclopedia of nanoscience and nanotechnology. New York: Marcel Dekker, Inc; 2004 p. 3015–3030.
[4] Noval B. Adv Mater 1993;5:422–33.
[5] Burnside SD, Giannelis EP. Chem Mater 1995;7:1597–600.
[6] Vaia RA, Giannelis EP. Macromolecules 1997;30:8000–9.
[7] Park J, Jana SC. Macromolecules 2003;36:2758–68.
[8] Park J, Jana SC. Macromolecules 2003;36:8391–7.
[9] Park J, Jana SC. Polymer 2004;45:7673–9.
[10] Mehta S, Mirabella FM, Rufener K, Bafna A. J Appl Polym Sci 2004;92:928–36.

[11] Huang X, Lewis S, Brittain WJ, Vaia RA. Macromolecules 2000;33:2000–4.
[12] Lee KM, Han CD. Macromolecules 2003;36:7165–78.
[13] Choi S, Lee KM, Han CD. Macromolecules 2004;37:7649–62.
[14] Park JH, Jana SC. Polymer 2003;44:2091–100.
[15] Wang S, Hu Y, Wang Z, Yong T, Chen Z, Fan W. Polym Degrad Stab 2003;80:157–61.
[16] Lee DC, Jang LW. J Appl Polym Sci 1996;61:1117–22.
[17] Chen G, Chen X, Lin Z, Yao KJ. J Mater Sci Lett 1999;18:1761–3.
[18] Okamoto M, Moritta S, Taguchi H, Kim YH, Kotaka T, Tateyama H. Polymer 2000;41:3887–90.
[19] Kim JW, Jang LW, Choi HJ, Jhon MS. J Appl Polym Sci 2003;89:821–7.
[20] Lee S-S, Lee CS, Kim M-H, Kwak SY, Park M, Lim S, et al. J Appl Polym Sci 2001;39:2430–5.
[21] Chu L-L, Anderson SK, Harris JD, Beach MW, Morgan AB. Polymer 2004;45:4051–61.
[22] Kambour RP, Bendler JT, Bopp RC. Macromolecules 1983;16:753–7.
[23] Paul DR, Barlow JW. Polymer 1984;25:487–94.
[24] Suess M, Kressler J, Kammer HW. Polymer 1987;28:957–60.
[25] Nishimoto N, Keskkula H, Paul DR. Polymer 1989;30:1279–86.
[26] Cowie JMG, Reid VMC, McEwen IJ. Polymer 1990;31:486–9.
[27] Fowler ME, Keskkula H, Paul DR. Polymer 1987;28:1703–11.
[28] Fowler ME, Barlow JW, Paul DR. Polymer 1987;28:2145–50.
[29] McMaster LP. Adv Chem Ser 1975;142:43.
[30] Naito K, Johnson GE, Allara DL, Kwei TK. Macromolecules 1977;10:681–6.
[31] Du M, Gong J, Zheng Q. Polymer 2004;45:6725–30.
[32] Ougizawa T, Madbouly SA, Inoue T. Macromol Symp 2000;149:69–74.
[33] Fornes TD, Hunter DL, Paul DR. Macromolecules 2004;37:1793–8.
[34] Tanaka G, Goettler LA. Polymer 2002;43:541–53.
[35] Xie W, Gao Z, Pan W-P, Hunter D, Singh A, Vaia R. Chem Mater 2001;13:2979–90.
[36] Jang BN, Wang D, Wilkie CA. Macromolecules 2005;38:6533–43.
[37] Lee KM, Han CD. Macromolecules 2003;36:804–15.
[38] Pattanayak A, Jana SC. Polymer 2005;46:3394–406.